Int. J. Heat Mass Transfer. Vol. 23, pp. 559–56..

0017-9310/80/0401-0559 $02.00/0

SHORTER COMMUNICATIONS

PARALLEL-FLOW AND COUNTER-FLOW CONDENSATION ON AN INTERNALLY COOLED VERTICAL TUBE

M. FAGHRI*
Department of Mechanical Engineering,
Tehran University of Technology, Tehran, Iran
and
E. M. SPARROW
Department of Mechanical Engineering, 125 Mechanical Engineering, 111 Church St. S.E.,
University of Minnesota, Minneapolis, Minnesota, MN 55455, U.S.A.

(*Received* 11 *May* 1979 *and in revised form* 25 *June* 1979)

NOMENCLATURE

- c_p, specific heat;
- g, acceleration due to gravity;
- h, coolant heat-transfer coefficient;
- k, thermal conductivity;
- L, length of tube;
- $\dot{m}_1$, coolant flow rate;
- Pr, Prandtl number;
- Q, heat-transfer rate;
- Q_{max}, maximum value of Q, equation (15);
- Q_{CF}, counter-flow heat-transfer rate;
- Q_{PF}, parallel-flow heat-transfer rate;
- R, thermal resistance, equation (2);
- Re, coolant Reynolds number;
- r_i, inner radius of tube;
- r_o, outer radius of tube;
- T, coolant bulk temperature;
- T_e, exit bulk temperature;
- T_o, inlet bulk temperature;
- T_{sat}, temperature of saturated vapor;
- X, dimensionless axial coordinate, equation (11);
- X_L, value of X at $x = L$;
- x, axial coordinate, Fig. 1.

Greek symbols

- β, thermal resistance parameter, equation (12);
- δ, thickness of condensate layer;
- θ, dimensionless temperature, equation (11);
- θ_e, value of θ at coolant exit;
- λ, latent heat of condensation;
- μ, viscosity;
- ρ, density.

Subscripts

- 1, coolant;
- 2, condensate layer;
- w, wall.

INTRODUCTION

IN CONVENTIONAL analyses of parallel-flow or counter-flow heat exchangers, the heat-transfer coefficients of the participating fluid flows are assumed to be constant along the length of the exchanger. The only exception to this practice is the Colburn analysis (see for example, [1] pp. 453–457) in which the overall heat-transfer coefficient is assumed to vary linearly with temperature. There are instances, however, in which the nature of the heat-transfer process in one or both of the flows dictates a streamwise variation of the transfer coefficient. For instance, the thickening of a flowing liquid film owing to condensation will decrease the transfer coefficient. In this Communication, parallel-flow and counter-flow heat exchange involving a process-dictated transfer coefficient variation will be analyzed. Particular emphasis will be placed on the comparison between parallel-flow and counter-flow.

The physical problem to be studied here is the condensation of a pure saturated vapor on the external surface of a vertical tube which is internally water cooled. A schematic view of the problem is presented in Fig. 1. The left-hand diagram depicts the situation in which the downward direction of the coolant flow parallels the flow direction of the gravity-driven condensate film. In the right-hand diagram, the coolant flow is upward, which is in counter-flow to the condensate film.

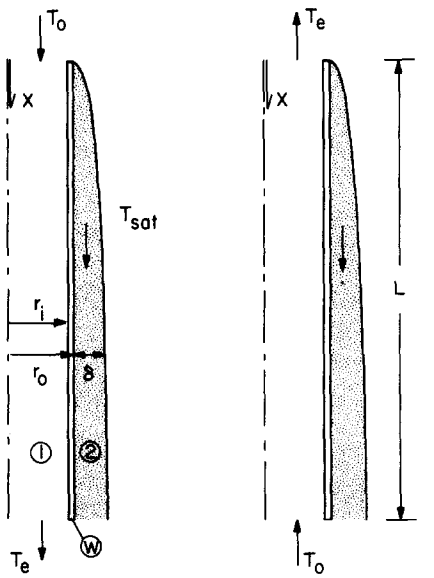

FIG. 1. Illustration of the physical problem. Left-hand diagram: parallel-flow. Right-hand diagram: counter-flow.

*Work performed when the author was an adjunct associate professor at the University of Minnesota.

In either case, the coolant temperature varies along the flow passage and, consequently, so do the wall temperature and the temperature difference across the condensate film. Since the growth of the condensate film depends on the aforementioned temperature difference, the heat-transfer coefficient for the film and its axial variation are determined by the dynamics of the heat-transfer process and cannot be specified *a priori*. It is this special feature which distinguishes the present problem from parallel-flow or counter-flow situations for which an *a priori* given transfer coefficient can be employed. With regard to the condensation problem treated here, it differs in a fundamental way from the classical Nusselt problem in that the temperature of the wall which bounds the condensate film cannot be specified in advance.

ANALYSIS

The various ingredients needed for the analysis will now be assembled. At any axial position x, the rate of heat transfer (for axial length dx) passing inward from the condensate to the coolant is

$$dQ = \frac{(T_{sat} - T)dx}{\frac{1}{h2\pi r_i} + \frac{\ln(r_o/r_i)}{2\pi k_w} + \frac{\delta}{k_2 2\pi r_o}} \tag{1}$$

where the three terms dividing the temperature difference are the respective thermal resistances for internal convection, wall conduction, and external condensation. In this equation, $T = T(x)$ is the local bulk temperature of the coolant, and h is the turbulent forced convection heat-transfer coefficient for pipe flow. The latter can be assumed independent of x because of the very short thermal entrance lengths for turbulent liquid flows and also because the transfer coefficients for turbulent pipe flows are generally insensitive to the thermal boundary condition at the wall. Curvature effects have been ignored in the last term of the equation because of the extreme thinness of the film.

It is convenient to lump the x-independent portion of the thermal resistance and to define

$$R \equiv r_o/r_i h + r_o \ln(r_o/r_i)/k_w, \tag{2}$$

so that

$$dQ = \frac{(2\pi r_o\, dx/R)(T_{sat} - T)}{1 + (\delta/Rk_2)}. \tag{3}$$

By use of the Nusselt theory of condensation (e.g. [2] pp. 533–536) the heat-transfer rate across the film (which is also equal to dQ) can be related to the film thickness δ via

$$dQ = (\rho_2^2 \lambda g/\mu_2) 2\pi r_o \delta^2 d\delta. \tag{4}$$

Also, by application of energy conservation to the coolant, another expression for dQ follows as

$$dQ = \pm \dot{m}_1 c_{p1} dT, \tag{5}$$

where the plus sign applies for parallel-flow and the minus sign is for counter-flow.

Equations (3)–(5) provide the vehicle for determining the variations of T and δ along the length of the tube as well as for finding Q. By bringing together (4) and (5) and integrating, there is obtained

$$\delta^3 = \pm \Omega^3 T + \text{constant}, \tag{6}$$

where Ω^3 is a convenient abbreviation (to be discarded shortly) for the constant factors in equations (4) and (5). To determine the integration constant in equation (6), information about δ and T has to be supplied at some axial station. For parallel-flow, it is known that $\delta = 0$ and $T = T_o$ at $x = 0$ (see left-hand diagram of Fig. 1), so that equation (6) becomes

$$\delta = \Omega(T - T_o)^{1/3}. \tag{7}$$

The counter-flow case is less convenient to deal with, since δ is known at $x = 0$ while T is known at $x = L$ (right-hand diagram of Fig. 1). To circumvent this difficulty cosmetically, tentative use will be made of the unknown coolant exit temperature T_e, and equation (6) will be evaluated using $\delta = 0$ and $T = T_e$ at $x = 0$, so that

$$\delta = \Omega(T_e - T)^{1/3}. \tag{8}$$

Then, the dQ terms are eliminated from equations (3) and (5), δ is introduced from either (7) or (8), and a dimensionless temperature θ and dimensionless coordinate X are employed. From these operations, there results

$$\frac{d\theta}{dX} = \frac{1 - \theta}{1 + \beta\theta^{1/3}} \quad \text{(parallel-flow)}, \tag{9}$$

$$\frac{d\theta}{dX} = -\frac{1 - \theta}{1 + \beta(\theta_e - \theta)^{1/3}} \quad \text{(counter-flow)}, \tag{10}$$

where

$$\theta = \frac{T - T_o}{T_{sat} - T_o}, \quad X = \frac{2\pi r_o x}{R\dot{m}_1 c_{p1}} = \frac{x/r_i}{Re_1 Pr_1} \frac{4r_o}{Rk_1}, \tag{11}$$

$$\beta = \left[\frac{3\dot{m}_1 c_{p1}\mu_2 (T_{sat} - T_o)}{\lambda \rho_2^2 g 2\pi r_o (Rk_2)^3}\right]^{1/3} = \left[\frac{3Re_1 Pr_1 k_1 \mu_2 r_i (T_{sat} - T_o)}{4\lambda \rho_2^2 g r_o (Rk_2)^3}\right]^{1/3} \tag{12}$$

and, when the tube wall resistance can be neglected,

$$X = \frac{2(x/r_i)Nu_1}{Re_1 Pr_1}, \quad Nu_1 = \frac{h(2r_i)}{k_1}. \tag{13}$$

The dimensionless bulk temperature distributions for either parallel-flow or counter-flow are governed by first-order ordinary differential equations, (9) and (10) respectively, which contain a single (albeit complex) parameter β. The quantity θ_e, the dimensionless exit temperature, is a computational input for the counter-flow case but not a true parameter.

Equations (9) and (10) have to be solved numerically, but the solution methodology is quite different in the two cases. For parallel-flow, starting with $\theta = 0$ at $X = 0$, equation (9) can be forward integrated (via the Runge–Kutta scheme) through a succession of X values. The integration can be continued at will, and any X along the way can serve as the exit cross section of the tube, and the θ value at each X can be regarded as the exit temperature.

For the counter-flow case, the computational scheme calls for the exit temperature θ_e to be selected and supplied to equation (10). The computations are then initiated at $X = 0$ and are continued through increasing X values until a station is encountered where $\theta = 0$. This station can be regarded as the tube inlet, and the corresponding X value is the dimensionless tube length X_L. Thus, unlike the parallel-flow case where a single computer run yields results for a host of tube lengths, a separate computer run must be made for each tube length in the counter-flow case.

RESULTS AND DISCUSSION

The quantity of most direct utility is the heat-transfer rate Q, which can be expressed as

$$Q = \dot{m}_1 c_{p1}(T_e - T_o). \tag{14}$$

The maximum possible rate of heat transfer Q_{max} is attained when $T_e = T_{sat}$, so that

$$Q_{max} = \dot{m}_1 c_{p1}(T_{sat} - T_o), \quad Q/Q_{max} = (T_e - T_o)/(T_{sat} - T_o). \tag{15}$$

Thus, the Q/Q_{max} ratio, which is sometimes called the heat exchanger effectiveness, can be represented as the temperature ratio $(T_e - T_o)/(T_{sat} - T_o)$.

The heat-transfer results for the parallel-flow case are

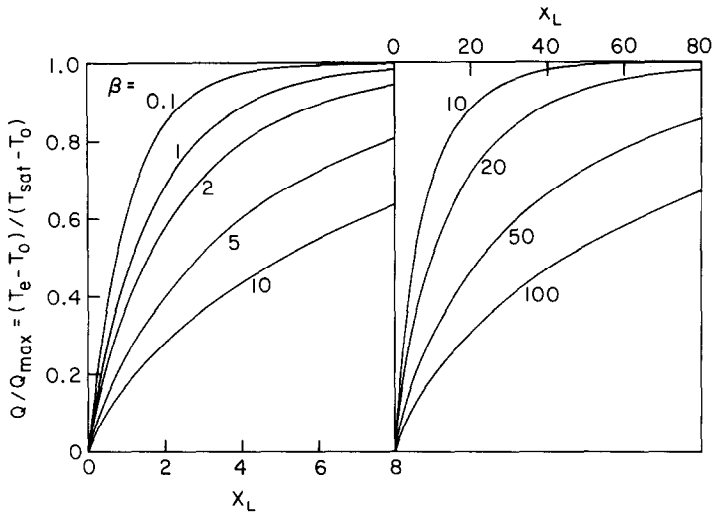

FIG. 2. Heat transfer results for parallel-flow.

presented in Fig. 2, where Q/Q_{max} is plotted as a function of the dimensionless tube length X_L. The curves are parameterized by the β parameter ranging between 0.1 and 100, with those curves for small and intermediate β displayed in the left-hand graph and the remainder displayed in the right-hand graph.

Figure 2 confirms the expected trend whereby the rate of heat transfer increases as the length of the tube increases. The extent of the increase in Q is most marked for relatively short tubes. For longer tubes, the increase of Q with length is more gradual. This behavior may be related to two causes. First, the temperature difference $T_{sat} - T$ is largest near $X = 0$ and decreases with increasing X. Second, since the condensate layer thickness δ is smallest at $X = 0$ and increases with X, the overall thermal resistance for radial heat flow also increases. These two factors work together to produce locally high rates of heat transfer at small X and lower rates at larger X. The variation of the thermal resistance is a special feature of the present analysis that is not found in conventional parallel-flow or counter-flow analyses.

Attention will now be focused on the role of the β parameter. From an examination of equations (3) and (9), it is evident that $\beta\theta^{1/3}$ is the ratio of the thermal resistance of the condensate film to the resistance R [equation (2)] of the tube wall and the coolant. The overall resistance is $(1 + \beta\theta^{1/3})$. Thus, for small β, the overall resistance is small and the consequent high rates of local heat transfer cause a rapid rise of the coolant temperature. On the other hand, high β signals a high thermal resistance, with lower local heat transfer rates and a more gradual rise in coolant temperature. These characteristics are reflected in Fig. 2 and also explain why the left-hand graph (smaller β) is accorded a much smaller range of X_L than is the right-hand graph.

Next, turning to the counter-flow case, a presentation of heat transfer results can readily be made in a form similar to Fig. 2 for parallel-flow. However, this information can be conveyed in a more meaningful way via a comparison of the parallel-flow and counter-flow results. To this end, the ratio Q_{CF}/Q_{PF} is plotted in Fig. 3 as a function of the dimensionless tube length, with β as the curve parameter. The comparisons shown in the figure are for common tube lengths and common coolant flow rates for the two cases.

All of the curves display a common pattern. At very short tube lengths $Q_{CF}/Q_{PF} = 1$, then, as the tube length increases, the curves rise, attain a maximum, and then diminish toward $Q_{CF}/Q_{PF} = 1$. Of particular interest is the height of the maximum since it indicates the maximum advantage of counter-flow compared with parallel-flow for a given β. The figure shows that the maximum value of Q_{CF}/Q_{PF} increases with β. For intermediate β (β = 1–10), Q_{CF}/Q_{PF} ranges from

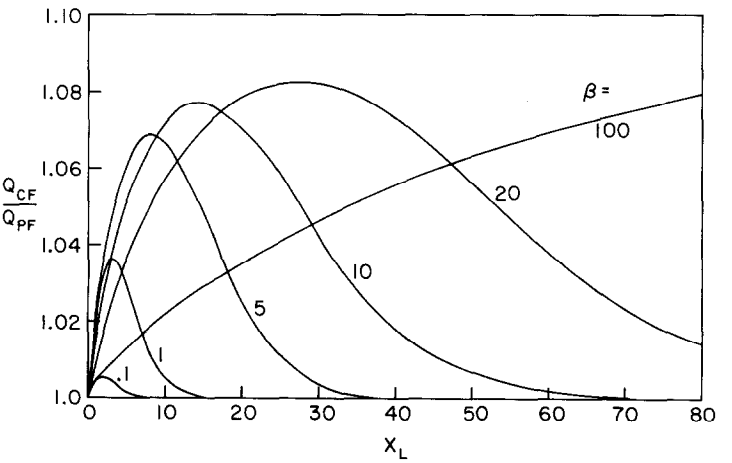

FIG. 3. Comparison of heat transfer results for parallel-flow and counter-flow.

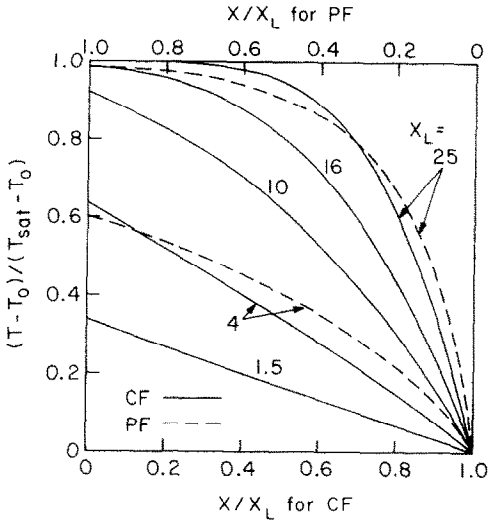

FIG. 4. Representative coolant temperature distributions, $\beta = 5$.

about 1.035 to 1.075. Thus, in broad terms, the counter-flow arrangement yields about a 5% heat transfer advantage relative to parallel-flow. Such an advantage can be regarded as modest.

That counter-flow is advantageous is by no means surprising, but the existence of a maximum in the Q_{CF}/Q_{PF} curves is interesting. The maximum can be made plausible by explaining why $Q_{CF}/Q_{PF} = 1$ at both small and large values of X_L. As $X_L \to 0$, the coolant is isothermal during its passage through the tube, and the flow direction is, therefore, immaterial. For large X_L, the coolant becomes thermally saturated, i.e. $T = T_{sat}$, so that once again the flow direction is of no consequence. At operating conditions other than these limits, Q_{CF} must exceed Q_{PF}, thereby giving rise to a maximum in the curve of Q_{CF}/Q_{PF} vs X_L. With increasing β, thermal saturation occurs at larger X_L, so that the curves shift to the right and upward.

To complete the presentation, attention is briefly focused on the coolant temperature distribution. For the parallel-flow case, Fig. 2 already conveys this information provided that the ordinate variable is regarded as $(T - T_o)/(T_{sat} - T_o)$ and the abscissa is regarded as X $(< X_L)$. Figure 4 shows representative temperature distributions for counter-flow (solid lines), where the curve parameter is X_L, and the results are for $\beta = 5$. The temperature increases in the flow direction as expected (right to left on the abscissa), and thermal saturation is in evidence for the case of $X_L = 25$. For comparison purposes, the figure also contains a few curves (dashed lines) for parallel-flow, plotted with respect to an oppositely increasing abscissa to facilitate the comparison. The figure shows that relative to the respective flow directions, the coolant temperature initially rises faster for parallel-flow, but counter-flow catches up and finally forges ahead because of its more efficient transfer properties in the downstream portion of the tube.

Acknowledgements — This research was supported in part by NSF grant ENG 75-18141 A01, and in part by the Iranian Ministry of Higher Education.

REFERENCES

1. D. Q. Kern and A. D. Kraus, *Extended Surface Heat Transfer*. McGraw-Hill, New York (1972).
2. B. V. Karlekar and R. M. Desmond, *Engineering Heat Transfer*. West Publishing, St. Paul (1977).

Int. J. Heat Mass Transfer. Vol. 23, pp. 562–566
Pergamon Press Ltd. 1980. Printed in Great Britain

DETERMINATION DE LA DIFFUSIVITE ET DE LA CHALEUR MASSIQUE PAR TRAITEMENT D'UNE EVOLUTION THERMOCINETIQUE TRANSITOIRE

P. THERY, J. P. DUBUS et F. WATTIAU*

(*Recu le* 22.2.79. *Version révisé le* 4.10.79)

NOMENCLATURE

a', a'_s,	diffusivités;
c, c', C,	chaleurs massiques, capacité thermique;
e, L, ε, x,	longueurs, variables d'espace;
t, J, p,	temps, constante de temps, variable de Laplace;
K,	coefficient de transfert;
$J(t)$,	quantité de chaleur;
$\Phi_1, \Phi_2, \Phi'_1, \Phi'_2$,	flux calorifiques;
$\Sigma\Phi, \Delta\Phi$,	combinaisons de flux calorifiques;
$T_0, T'_0, T_1, T'_1, T_2, T'_2$,	températures;
$\Delta T, \Sigma T$,	combinaisons de températures;
ρ, ρ',	masses volumiques;
λ, λ',	conductivités thermiques;
AA', BB',	plans de section droite;
E, E_1, E_2,	tensions électriques;
s, d,	expressions de la réponse.

* Universite des Sciences et Techniques de Lille.
Cresmat, Centre de Recherche Science des Matériaux et Techniques de Construction, Bâtiment P3 – 3è Etage, 59655—Villeneuve d'Ascq Cédex, France.